PHYSICAL REVIEW D **72,** 112001 (2005)

Formation length effects in very thin targets

U. I. Uggerhøj,[1] H. Knudsen,[1] S. Ballestrero,[2] P. Sona,[2] A. Mangiarotti,[3] T. J. Ketel,[4] A. Dizdar,[5] S. Kartal,[5] and C. Pagliarone[6]

[1]*Department of Physics and Astronomy, University of Aarhus, Denmark*
[2]*University of Florence, Florence, Italy*
[3]*Physikalisches Institut, Heidelberg, Germany*
[4]*Free University, Amsterdam, The Netherlands*
[5]*University of Istanbul, Istanbul, Turkey*
[6]*University of Cassino, Italy and INFN Pisa, Italy*

(Received 10 May 2005; published 12 December 2005)

Experimental results for the radiative energy loss of 178 GeV positrons in Cu, Au, and W targets are presented. It is shown that for a few micron thick target, effects related to the formation zone disappear, in particular, the suppression due to the Landau-Pomeranchuk-Migdal and Ternovskii-Shul'ga-Fomin mechanisms. This disappearance may restrict the region of applicability of thin foils as a target for energy-selective production of high energy photons. Furthermore, transition radiation dominated by multiple scattering and structured target interference effects are shown to be likely ingredients for an accurate description of the data obtained at low photon energies.

DOI: 10.1103/PhysRevD.72.112001 PACS numbers: 41.60.−m, 07.85.Fv, 29.40.Vj, 95.30.Gv

I. INTRODUCTION

In the bremsstrahlung emission from an energetic positron or electron traversing a solid, there are four basic scales of length: The radiation length X_0, the foil thickness Δt, the formation length $l_f = 2\gamma^2 c(E - \hbar\omega)/E\omega$, and the 'multiple scattering length' $l_\gamma = \alpha/4\pi \cdot X_0$, where $E = \gamma mc^2$ and $\hbar\omega$ are the energy of the positron and photon, respectively, m is the rest mass of the positron, γ the Lorentz factor, α the fine-structure constant, and c the speed of light. Of these lengths, the only one that depends on photon and particle energy is the formation length, whereas the other lengths depend on the target material or shape.

In earlier papers [1,2], measurements of the Landau-Pomeranchuk-Migdal (LPM) effect were presented—a suppression of radiation yield from electrons with energies in the few hundred GeV range. The LPM effect can be interpreted as a disturbance of the projectile within the formation length that leads to a reduced radiation probability. In other words, the suppression appears if the formation length exceeds the multiple scattering length, but remains smaller than the target thickness, i.e. $l_\gamma < l_f < \Delta t$. Since the formation length is inversely proportional to the energy of the radiated photon, low energy photons suffer a stronger suppression than high energy ones for fixed energy of the particle. Furthermore, for particle energies of around 200 GeV, the formation length for a 20 GeV photon becomes a few microns long, i.e. in the experimentally accessible regime for the experimental use of thin targets in high energy beams. Likewise, for heavy materials the multiple scattering length becomes a few microns. In experiments performed at SLAC, the case $l_\gamma < \Delta t < l_f$ has been studied [3–5] where the formation length loosely speaking extends out of the target while the target is thick enough to yield a typical scattering angle exceeding $1/\gamma$. In this case, a new type of suppression phenomenon appears, first treated theoretically by Ternovskii [6] and later in substantial detail by Shul'ga and Fomin [5,7–11].

The present study is aimed at providing an experimental answer to the question: what happens to formation zone effects once the available target thickness becomes comparable to the multiple scattering length which in turn is smaller than the formation length, i.e. when $l_\gamma \simeq \Delta t < l_f$? Theoretically, the target will act as a single scatterer and will produce radiation according to the unsuppressed Bethe-Heitler mechanism even though $l_f > l_\gamma$ [10]. Secondly, transition radiation in the multiple scattering dominated regime turns out to give a significant contribution to the radiation in the few GeV region.

II. THEORY

The basic formulas for the various radiation effects considered are briefly presented. For more comprehensive discussions the reader is referred to other texts [2,12].

A. Landau-Pomeranchuk-Migdal effect

Since the majority of radiation emission takes place within a cone of opening angle $1/\gamma$ to the direction of the electron, loss of coherence during the formation time results in suppression if the electron scatters outside this cone. So if half (in the convention of [12]) the formation length exceeds the length l_γ, the emission probability decreases, i.e. an onset of the LPM effect at energies:

$$\hbar\omega_{\mathrm{LPM}} = \frac{E^2}{E + E_{\mathrm{LPM}}}, \tag{1}$$

where $E_{\mathrm{LPM}} = mc^2 X_0/4\pi a_0 = 7.68 \cdot X_0$ TeV/cm and a_0 is the Bohr radius.

The LPM effect in finite size targets was treated theoretically in detail by e.g. Blankenbecler and Drell [13], by Zakharov [14], and by Baier and Katkov [15].

B. Thin target—Ternovskii-Shul'ga-Fomin effect

Because the formation length for radiation emission increases with decreasing photon frequency, at a certain point the formation zone extends beyond the thickness of the foil. In this case, the radiation yield also becomes suppressed. Theoretical studies of this effect were first performed by Ternovskii [6] and later extended by Shul'ga and Fomin [5,7–11]. The phenomenon is also of substantial interest in QCD [16–19].

For the Ternovskii-Shul'ga-Fomin (TSF) effect, the analysis is applicable for target thicknesses $l_\gamma \ll \Delta t < l_{\mathrm{f}}$, see e.g. [10]. Combining the formation length and the target thickness parametrized by $k_{\mathrm{f}} > 1$, $\Delta t = l_{\mathrm{f}}/k_{\mathrm{f}}$, the effect becomes appreciable for photon energies

$$\hbar\,\omega < \hbar\omega_{\mathrm{TSF}} = \frac{E}{1 + \frac{\Delta t}{2\gamma\lambda_c}}, \tag{2}$$

where $\lambda_c = \hbar/mc$ is the (reduced) Compton wavelength.

The magnitude of the effect is evaluated from the averaged radiation spectrum [10]

$$\left\langle \frac{\mathrm{d}E}{\mathrm{d}\omega} \right\rangle \simeq \frac{2\alpha}{\pi}\left(\ln\left(\frac{\Delta t}{l_\gamma}\right) - 1\right) \tag{3}$$

and since for the Bethe-Heitler case $\langle \frac{\mathrm{d}E}{\mathrm{d}\omega} \rangle = 4\Delta t/3X_0$, the suppression factor κ can conveniently be expressed as

$$\kappa \simeq \frac{k_\gamma}{6(\ln k_\gamma - 1)}, \tag{4}$$

where $\Delta t = k_\gamma l_\gamma$ and $k_\gamma \gg 1$ ensures $\Delta t \gg l_\gamma$. As an example, for $\Delta t = 0.3\% X_0$, corresponding to a 10 μm thin Au target and $E = 178$ GeV, $k_\gamma \simeq 5$ yielding a suppression $\kappa = 1.3$ for photon energies lower than $\hbar\omega_{\mathrm{TSF}} = 4.7$ GeV.

At higher energies, as the Lorentz factor γ becomes comparable to $\Delta t/2\lambda_c$ the suppression affects a substantial part of the spectrum. At 4 TeV—perhaps relevant for a tertiary beam derived from the LHC beam [20]—the effect suppresses the lower half of the radiation spectrum by a factor 2 in a 7 μm thick Au foil. The effect may thus be an alternative to coherent bremsstrahlung from a crystal to enhance the production of high energy photons from a target. However, if the theory is correct, the suppression should disappear once the target no longer fulfills $\Delta t \gg l_\gamma$ since the radiation will reenter the regime of the Bethe-Heitler type.

C. Transition radiation

Following the discussion in [21] there are two different regimes of emission of transition radiation corresponding to the requirements $E < E_0$ or $E > E_0$, where $E_0 \simeq \omega_p l_\gamma mc$ separates the two regions according to whether or not multiple scattering is important. Here ω_p is the plasma frequency yielding $E_0 \simeq 0.4$ GeV for Au where $\omega_p \simeq 80$ eV. In the region $E < E_0$ the number of photons emitted per edge is given by the ''standard'' expression (see e.g. [22])

$$\frac{dN}{d\hbar\omega} = \frac{\alpha}{\pi\hbar\omega}\left[\left(1 + \frac{2\omega^2}{\gamma^2\omega_p^2}\right)\ln\left(1 + \frac{\gamma^2\omega_p^2}{\omega^2}\right) - 2\right] \tag{5}$$

while in the region $E > E_0$ the number of photons emitted per edge is given by

$$\frac{dN}{d\hbar\omega} \approx \frac{\alpha}{\pi\hbar\omega}\left[\ln\left(\frac{1 + \sqrt{1 + 4\omega_{\mathrm{LPM}}/\omega}}{2}\right) + \frac{2}{1 + \sqrt{1 + 4\omega_{\mathrm{LPM}}/\omega}} - 1\right] \tag{6}$$

which is valid for $\hbar\omega > \gamma\hbar\omega_p$ and a not too thin foil.

These expressions approximately agree for energies smaller than $\simeq 0.1\gamma\hbar\omega_p$ corresponding to 2.8 MeV in Au. For an energy $\hbar\omega = 5$ GeV in 2 μm Au, Eq. (5) multiplied by $2X_0/\Delta t$, i.e. normalized to thickness and taking entry and exit edge into account, gives $dN/d\hbar\omega = 10^{-11}$ GeV^{-1}. For the same conditions, Eq. (6) gives $dN/d\hbar\omega \approx 0.34$ GeV^{-1}. Both conditions $E > E_0$ and $\hbar\omega > \gamma\hbar\omega_p$ are fulfilled by a reasonable margin. This can be compared with an alternative treatment [23] (see also [4]) valid for photon energies $\gamma\hbar\omega_p(\gamma\hbar\omega_p/\hbar\omega_{\mathrm{LPM}})^{1/3} < \hbar\omega \ll \hbar\omega_{\mathrm{LPM}}$, corresponding to 4 MeV $< \hbar\omega \ll 11.5$ GeV in Au

$$\frac{dN}{d\hbar\omega} = \frac{\alpha}{\pi\hbar\omega}\ln\left(\frac{2}{3}\sqrt{\frac{\hbar\omega_{\mathrm{LPM}}}{\hbar\omega}}\right) \tag{7}$$

which at $\hbar\omega = 5$ GeV yields $dN/d\hbar\omega \approx 0.019$ GeV^{-1}. In fact, [23] shows Eq. (6) with different numerical coefficients yielding a lower result $dN/d\hbar\omega \approx 0.22$ GeV^{-1}. Thus, it is not unreasonable to expect that Eq. (6)—which is anyway only approximate—may overestimate the yield of transition radiation.

A more recent theory of the multiple scattering dominated transition radiation is provided by Baier and Katkov [15]. Although rather compact, their expression (Eq. (4.9) [15]) requires the definition of a number of auxiliary

variables, and the reader is referred to the original publication for details. The yield is about a factor 2 higher than that given by Eq. (6). We have been unable to produce meaningful numbers from their equation (6.13) which should be applicable for our case and we encourage the ''detailed analysis of the probability of radiation in targets of intermediate thickness'' ($\Delta t \simeq l_f$) mentioned [15].

In any case, the analysis shows that transition radiation dominated by multiple scattering may be a necessary ingredient in the description for targets thick enough to yield this type of radiation.

D. Structured target theory

In Blankenbecler's theory [24,25] (see also [14]) interference mechanisms are considered for targets of up to 10 segments. It is shown that ''the photon spectrum is clearly developing a peak where the formation length is approximately equal to the distance between the centers of the plates'' [24]. Even though these calculations are performed only for 25 GeV (and in a single case 50 GeV), there seems to be no reason to expect that this observation does not apply to the general case.

In [26], Baier and Katkov treat the radiation emission from a stack of thin foils, including the LPM and polarization effect and emission from the target boundaries (transition radiation). For the general case of N foils, however, they only give an explicit formula for the strong scattering, large spacing case where, in their notation, $b \ll 1$ and $T = (l_1 + l_2)/l_f \gg 1$, l_1 being the target segment thickness, l_2 the segment spacing (their Eq. (2.49)), and $b = \alpha X_0/2\pi l_1$ the scattering variable.[1] In our case, $b = 2$ does not fulfill the requirement, and the length variable T is not much larger than 1 for photon energies in the interesting region, for instance $T = 2 - 7$ for $\hbar\omega = 3 - 10$ GeV with $l_2 = 30$ μm and 2 μm Au targets. For targets with $l_1 = 10$ μm and 20 μm the requirement on b is barely fulfilled. Moreover, in ([26] Eq. (2.49)) the additional radiation probability (apart from the single foil one with $T = 1$) for the large N case becomes proportional to $5.6(N-1)\cos T/Nb^2T^2$ times the Bethe-Heitler value. Therefore, very large values of T are required to extract meaningful numerical values. This does not mean that what seems to be a correct theory has not been fully developed by Baier and Katkov. However, it would be necessary to redo the rather involved calculation in the case $T \simeq 1$, $b \simeq 1$, $N \gg 1$, starting from their basic Eq. (2.30). In any case, the calculated interference maxima of Baier and Katkov agree with the above quoted rule and are thus not expected to be dominant in the present experiment. The reason is that the formation length for photon energies $\hbar\omega > 2.4$ GeV barely becomes equal to the shortest target spacing, 30 μm (which would equal the formation length at 1.6 GeV).

In [27] a similar setup is treated theoretically, although with emphasis on the low energy photons and the similarity between transition radiation from a structured target and undulator radiation.

[1]Using the definition of Q as a function of n as defined in [26] yields a value of b that is a factor Z too small. We have used the definition of n from [15].

III. EXPERIMENT

The experiment was performed in the H4 beamline of the CERN SPS using a tertiary beam of positrons with an energy of 178 GeV. The fraction of particles heavier than positrons in the beam is low, estimated to about 10^{-2}. In Fig. 1 we give a schematical overview of the setup adopted for the experiment. The incident positron beam is defined by a scintillator counter, S2, in combination with a scintillator veto with a Ø9 mm hole, $\overline{\text{S1}}$. In front of $\overline{\text{S1}}$ the target of about 4% X_0 is placed. The emitted photons are finally intercepted in a lead glass detector (LG), the low energy cutoff of which was set to 2.4 GeV in the analysis to avoid influence from the pedestal.

Because of the presence of scintillator and air in parts of the beamline, the background corresponds to about 3% X_0. Since a gold target of thickness comparable to l_γ must be of the order 2 μm (0.06% X_0) thick, a stacking technique was used to achieve a sufficient signal-to-background ratio, while maintaining a fixed distance between each pair of Au foils. The same technique could be used to investigate the radiation from structured targets [13,15]. The resulting so-called 'sandwich'-target consisted of 53 layers of 2 μm Au, interspersed with 30 μm of low density PolyEthylene (LDPE) mounted in a holder with an open area of 12×12 mm^2. Since the radiation length of LDPE is about 350 mm, corresponding to a total of 0.4% X_0 in the sandwich-target, the influence of the extra material thus introduced is marginal and the LDPE can to a first approximation be treated as air gaps.

Four target configurations were used (identified below by the label given in parenthesis): (Au2) The 53×2 μm sandwich-target with 30 μm LDPE spacers described above, (W20) a similar target of 4×20 μm W with 100 μm LDPE spacers, (Cu500) a 0.5 mm solid Cu target, and finally a rearrangement of the Au sandwich to (Au10) a $10 \times (5 \times 2)$ μm sandwich-target with 30 μm LDPE spacers, in effect making each subsection 10 μm in thickness. For each target except (Au10), two amplifications of the photo multiplier on the lead glass detector were employed. The first setting was used for all targets, where photon energies in the range 2–220 GeV could be read out and the second setting was used to magnify the low energy photon spectrum, reading only the 2–25 GeV lower part of the emitted photon energies. The background measured with an empty target has been subtracted from the data.

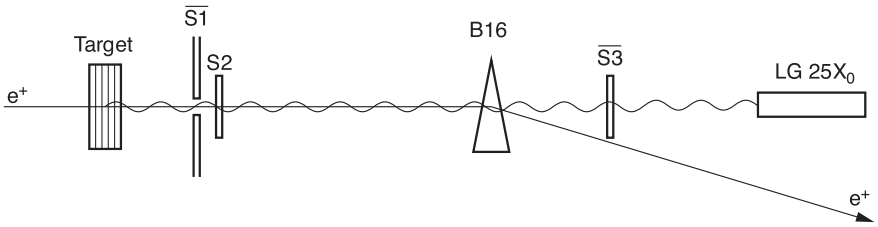

FIG. 1. A schematical drawing of the setup used in the experiment. The total length of the setup is about 21 m.

IV. RESULTS

In Fig. 2 we show the full radiation spectrum recorded for the Au2 target for both LG amplifications and compared to simulated values based on the nominal value for E_{LPM} (LPM) and E_{LPM} set to 10^9 GeV (Bethe-Heitler). In the simulations, only one homogeneous radiator volume was employed. The LPM effect was incorporated in the framework of the GEANT package as described in [2]. The vertical scale has been normalized to the thickness expressed in units of the radiation length. The thicknesses were evaluated by a least-squares fit using the LPM expression with the thickness as a free parameter. The values found were about 30% lower than the nominal thickness for the Au targets, reflecting the accuracy of the thickness in the production process, estimated to be about 20%.

There is a good agreement between theory and data for all energies down to $\simeq 5$ GeV. Below this value, a difference has been found, which is the main region of interest to be discussed.

In Figs. 3–6 we show the recorded power spectra for all targets, focusing on the region below $\hbar\omega = 20$ GeV. In all cases, the agreement with the simulated values is good down to an energy of about 5 GeV. For lower photon energies, the thinner targets show a clear tendency to exceed the simulated values including the LPM effect, tending towards the Bethe-Heitler values. Furthermore, this tendency becomes more pronounced the thinner the target, and in the Au2 case the experimental points even exceed the Bethe-Heitler values. For the Au2 and Au10 cases, the values of k_γ are only 1.0 and 5.1 which is hardly enough for the applicability of the TSF theory which requires $k_\gamma \gg 1$. Thus, we expect these targets to act approximately as "single scatterers," i.e. to give a radiation spectrum close to that of the Bethe-Heitler type.

The excess compared to the Bethe-Heitler value is likely to be partly due to transition radiation as discussed above. Replacing the coefficient 4 in Eq. (6) by 1 and reducing the yield by a factor 3 gives a reasonably close match to the excess appearing in Fig. 3. However, the statistical and systematic uncertainties of the experiment do not allow these theoretical values to be accurately extracted. Moreover, for photon energies approaching the experimental threshold, $\hbar\omega = 2.4$ GeV, the formation length reaches dimensions of the order of the target separation and structured target effects may contribute to the disappearance of the TSF effect.

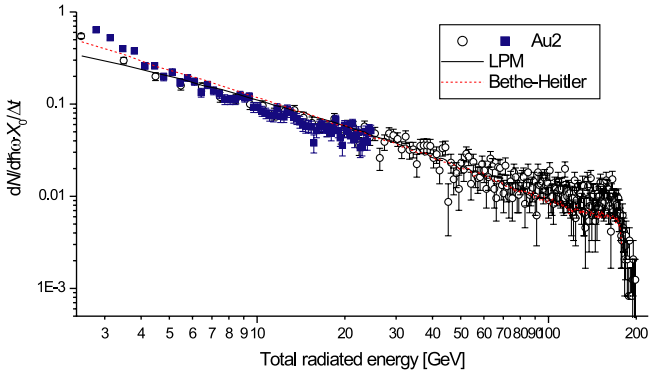

FIG. 2 (color online). Normalized bremsstrahlung spectrum, $dN/d\hbar\omega \cdot X_0/\Delta t$, for 178 GeV positrons on 53 layers of 2 μm Au with 30 μm LDPE spacers. The vertical scale is normalized to the number of incoming positrons and the thickness in units of the radiation length. The open dots represent the spectrum for low LG amplification, the filled squares for high amplification, the full line the simulated values including the LPM effect, and the dashed line the simulated values for the Bethe-Heitler mechanism.

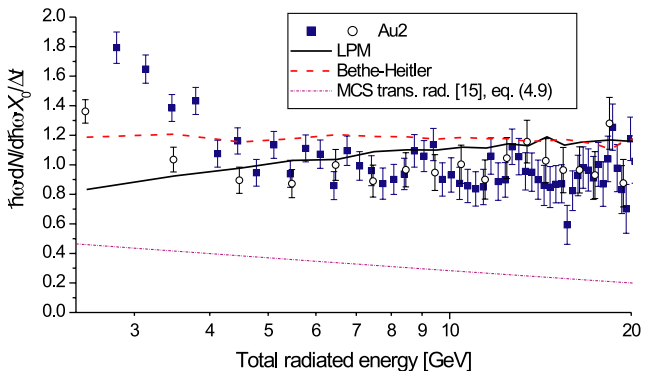

FIG. 3 (color online). Normalized bremsstrahlung power spectrum, $\hbar\omega dN/d\hbar\omega \cdot X_0/\Delta t$, for 178 GeV positrons on 53 layers of 2 μm Au with 30 μm LDPE spacers. The vertical scale is normalized to the number of incoming positrons and the thickness in units of the radiation length. The meaning of the symbols is as in Fig. 2. The additional line shows the contribution from multiple scattering dominated transition radiation according to ([15] Eq. (4.9)).

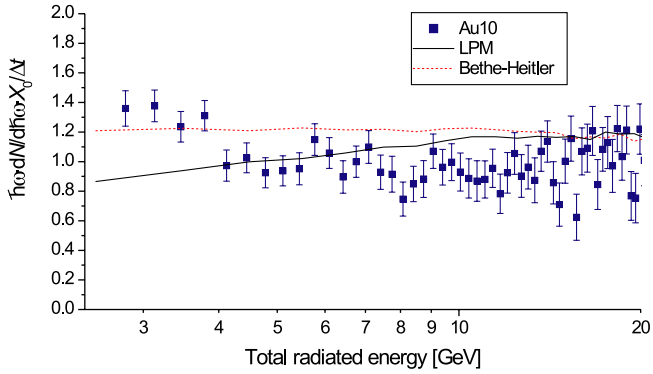

FIG. 4 (color online). Normalized bremsstrahlung power spectrum, $\hbar\omega dN/d\hbar\omega \cdot X_0/\Delta t$, for 178 GeV positrons on 10 layers of 5×2 μm Au with 30 μm LDPE spacers. The vertical scale is normalized to the number of incoming positrons and the thickness in units of the radiation length. The meaning of the symbols is as in Fig. 2.

For the W20 target, the TSF theory should be applicable, with $k_\gamma = 10$. However, in this case the suppression is relatively small, $\kappa \simeq 1.3$ and appears at just below the experimental threshold. We do therefore not expect evidence for the TSF effect in the present experiment.

We emphasize that the runs with low and high amplification were taken separately and the fact that they agree within the statistical uncertainty shows that systematic effects are unlikely to be responsible for the tendencies discussed. The low amplification data points, however, are consistently lower than the high amplification data points for small photon energies. This is likely to be due to the calibration of the high amplification data set, performed with positrons of only 2 energies, 10 and 20 GeV. The systematic uncertainty for this calibration has been evaluated to about 10%. However, as a result of the uncertainties connected to reading small signals from the lead glass photo multiplier for the low amplification data set, we believe the high amplification data points (filled squares in Figs. 2–6 to be the most reliable in the low photon energy region.

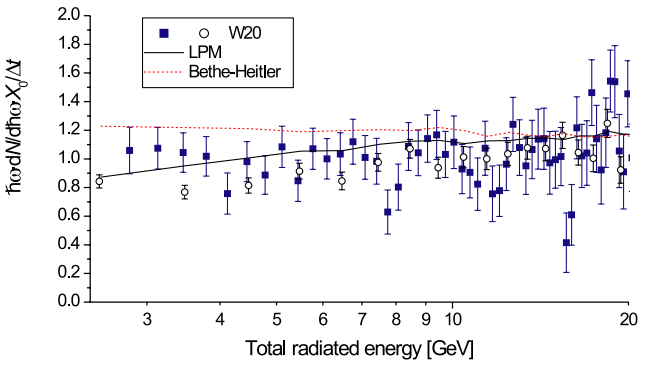

FIG. 5 (color online). Normalized bremsstrahlung power spectrum, $\hbar\omega dN/d\hbar\omega \cdot X_0/\Delta t$, for 178 GeV positrons on 4 layers of 20 μm W with 100 μm LDPE spacers. The vertical scale is normalized to the number of incoming positrons and the thickness in units of the radiation length. The meaning of the symbols is as in Fig. 2.

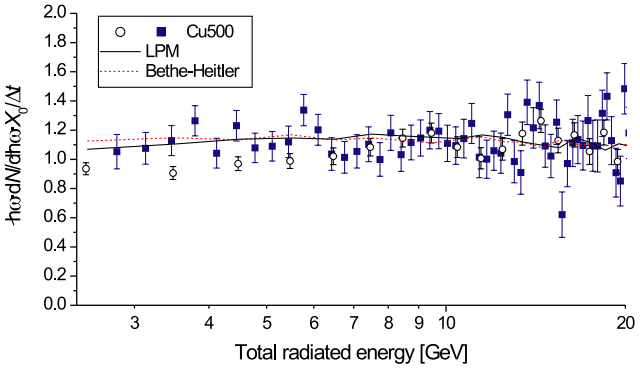

FIG. 6 (color online). Normalized bremsstrahlung power spectrum, $\hbar\omega dN/d\hbar\omega \cdot X_0/\Delta t$, for 178 GeV positrons on 0.5 mm Cu. The vertical scale is normalized to the number of incoming positrons and the thickness in units of the radiation length. The meaning of the symbols is as in Fig. 2.

The 'transition region' from the LPM effect back to the Bethe-Heitler mechanism as the target thickness is lowered, is around 4–5 GeV for a target of thickness comparable to $l_\gamma \simeq 2$ μm. This photon energy corresponds to a formation length of about 10 μm. It is unlikely that the effect is due to transition radiation alone since this contribution is reduced by more than a factor 5 going from the Au2 target to Au10. Finally it should be mentioned that the simple, but approximate form for l_γ as equal to $\alpha/4\pi \cdot X_0$ employed here, probably is too inaccurate for a detailed theoretical description of the phenomenon. Modifications of the expected scattering angle distributions as from e.g. [28,29] may lead to slightly different results for the onset of the TSF effect [30].

V. CONCLUSION

We have shown experimentally that for sufficiently thin targets arranged in a sandwich configuration, the LPM suppression mechanism related to the formation length disappears. The measurements are compared to simulations based on the Bethe-Heitler and Landau-Pomeranchuk-Migdal mechanisms for bremsstrahlung emission and a simplified treatment of the Ternovskii-Shul'ga-Fomin effect relevant for thin targets is shown to lead to an understanding of the "threshold" for the disappearance. Furthermore, transition radiation dominated by multiple scattering in the regime $E \gtrsim E_0$ as well as structured target interference effects are likely to be explanations for at least part of the discrepancy observed for the thinnest targets. More accurate calculations based on e.g. the theory of Baier and Katkov [15,26] of radiation in thin structured targets in this regime are called for, to resolve this question of the exact origin of the discrepancy.

ACKNOWLEDGMENTS

We are very grateful to Jacques Chevallier for producing the large number of 2μm thin Au foils in a short time and at a reasonable cost. Likewise, the strong support from P. B. Christensen and P. Aggerholm (DPA, Aarhus), I. Efthymiopoulos, and A. Fabich (CERN) is highly appreciated. Furthermore, we wish to thank Professors Shul'ga and Fomin for constructive criticism to the draft of this paper. U. I. U. and H. K. acknowledge support from the Danish Natural Science Research Council and S. K. acknowledges support from the Research Fund of Istanbul University Project No. 1755/21122001.

[1] H. D. Hansen *et al.*, Phys. Rev. Lett. **91**, 014801 (2003).
[2] H. D. Hansen *et al.*, Phys. Rev. D **69**, 032001 (2004).
[3] P. L. Anthony *et al.*, Phys. Rev. Lett. **75**, 1949 (1995).
[4] P. L. Anthony *et al.*, Phys. Rev. D **56**, 1373 (1997).
[5] N. F. Shul'ga and S. P. Fomin, JETP Lett. **63**, 873 (1996).
[6] F. F. Ternovskii, JETP **12**, 123 (1961).
[7] N. F. Shul'ga and S. P. Fomin, JETP **27**, 117 (1978).
[8] N. F. Shul'ga and S. P. Fomin, Phys. Lett. A **114**, 148 (1986).
[9] N. F. Shul'ga and S. P. Fomin, Nucl. Instrum. Methods Phys. Res., Sect. B **145**, 73 (1998).
[10] N. F. Shul'ga and S. P. Fomin, JETP **86**, 32 (1998).
[11] N. F. Shul'ga and S. P. Fomin, Nucl. Instrum. Methods Phys. Res., Sect. B **145**, 73 (1998).
[12] S. Klein, Rev. Mod. Phys. **71**, 1501 (1999).
[13] R. Blankenbecler and S. D. Drell, Phys. Rev. D **53**, 6265 (1996).
[14] B. G. Zakharov, JETP Lett. **64**, 781 (1996).
[15] V. N. Baier and V. M. Katkov, Phys. Rev. D **57**, 3146 (1998).
[16] B. G. Zakharov, Phys. At. Nucl. **61**, 838 (1998).
[17] B. Z. Kopeliovich, A. Schäfer, and A. V. Tarasov, Phys. Rev. C **59**, 1609 (1999).
[18] B. G. Zakharov, JETP Lett. **73**, 49 (2001).
[19] B. G. Zakharov, Nucl. Phys. B, Proc. Suppl. **146**, 151 (2005).
[20] E. Uggerhøj and U. I. Uggerhøj, Nucl. Instrum. Methods Phys. Res., Sect. B **234**, 31 (2005).
[21] M. L. Ter-Mikaelian, *High-Energy Electromagnetic Processes in Condensed Media* (Wiley Interscience, New York, 1972).
[22] J. D. Jackson, *Classical Electrodynamics* (John Wiley & Sons, New York, 1975).
[23] V. E. Pafomov, Sov. Phys. JETP **20**, 353 (1965).
[24] R. Blankenbecler, Phys. Rev. D **55**, 190 (1997).
[25] R. Blankenbecler, Phys. Rev. D **55**, 2441 (1997).
[26] V. N. Baier and V. M. Katkov, Phys. Rev. D **60**, 076001 (1999).
[27] V. N. Baier and V. M. Katkov, Nucl. Instrum. Methods Phys. Res., Sect. A **439**, 189 (2000).
[28] Particle Data Group, Phys. Lett. B **592**, 1 (2004).
[29] J. M. Corstens, W. Knulst, O. J. Luiten, and M. J. van der Wiel, Nucl. Instrum. Methods Phys. Res., Sect. B **222**, 437 (2004).
[30] N. F. Shul'ga and S. P. Fomin, private communication, 2005.